Finite element modeling of stress variation in multilayer thin-film specimens for in situ transmission electron microscopy experiments

H. Mei
Department of Aerospace Engineering and Engineering Mechanics, University of Texas, Austin, Texas 78712

J.H. An
Materials Science and Engineering Program, University of Texas, Austin, Texas 78712

R. Huang
Department of Aerospace Engineering and Engineering Mechanics, University of Texas, Austin, Texas 78712

P.J. Ferreira[a)]
Materials Science and Engineering Program, University of Texas, Austin, Texas 78712

(Received 28 January 2007; accepted 16 May 2007)

Multilayer thin-film materials with various thicknesses, compositions, and deposition methods for each layer typically exhibit residual stresses. In situ transmission electron microscopy (TEM) is a powerful technique that has been used to determine correlations between residual stresses and the microstructure. However, to produce electron transparent specimens for TEM, one or more layers of the film are sacrificed, thus altering the state of stresses. By conducting a stress analysis of multilayer thin-film TEM specimens, using a finite element method, we show that the film stresses can be considerably altered after TEM sample preparation. The stress state depends on the geometry and the interactions among multiple layers.

I. INTRODUCTION

Multilayer thin-film materials are used in many electronic and optoelectronic devices, wherein the thickness of each layer ranges from a few microns to several nanometers. With various chemical compositions and deposition methods used for each layer, multilayer thin films are normally subjected to residual stresses at room temperature.[1] In addition, these multilayers undergo thermal cycling during processing, and are subjected to changes in stress due to differences in the coefficients of thermal expansion for the various materials. These stresses are often detrimental to the performance of the aforementioned devices, leading to excessive substrate curvature, void formation and/or electromechanical failure.[2–4] Occasionally, the presence of stress and strain enhances performance of functional devices.[5] In either case, to optimize the application of multilayer thin films, it is crucial to understand the nature of residual stresses.

The use of in situ transmission electron microscopy (TEM) has been developed as one powerful technique in establishing a direct link between residual stresses and induced microstructural evolution in multilayer thin films.[6–9] The advent of electronic cameras and the continual development in electron optics and stage designs have greatly enhanced the capabilities of in situ TEM analyses. Currently, novel in situ experiments are able to observe and record micro-to-nanoscale behavior of materials in various heating, cooling, straining, or growth environments. These experiments are invaluable for characterizing and understanding thermomechanical properties along with the underlying dynamic processes.

Despite these advantages, there are usually concerns with in situ TEM experiments because to produce electron transparent specimens in these multilayers, one or more layers of the film need to be sacrificed, thus altering the state of the original residual stresses and potentially changing the operating stress-relief mechanisms. Past publications have described dislocation dynamics[8] and void formation behavior[9] in Cu under thermal stress conditions, which have significance in the microelectronic industry. While these reports provide valuable information on the microstructural changes that occur during stress evolution, they fail to discuss how the thinning of the TEM sample affects the stress state of the samples. If the original stress state has been altered due to sample

[a)]Address all correspondence to this author.
e-mail: reira@mail.utexas.edu
DOI: 10.1557/JMR.2007.0341

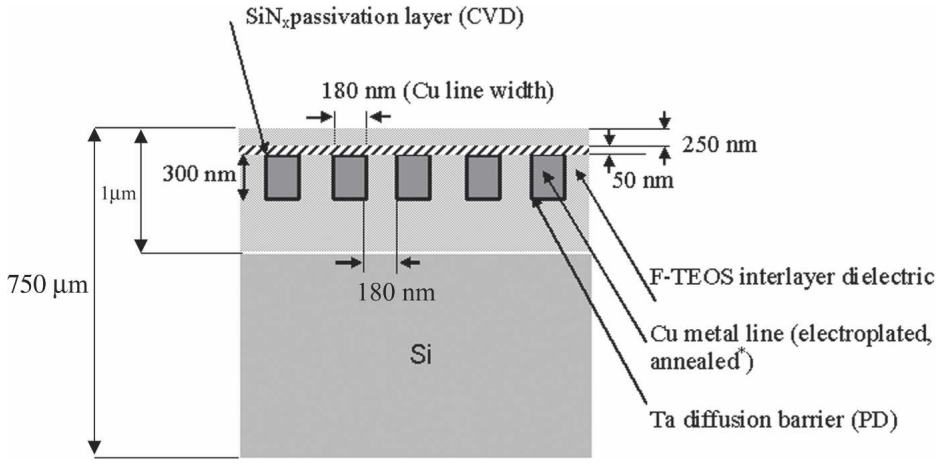

FIG. 1. Multilayer Cu interconnect structure.

thinning, the stress changes that occur in these samples would be different from those occurring in bulk samples. Thus, careful conclusions must be drawn from in situ TEM observations.

In this context, the objective of this paper is to conduct a systematic stress analysis of single-layer and multilayer thin-film specimens, which were thinned to electron transparency for in situ TEM experiments. In the past, convergent-beam electron diffraction (CBED) has been used to observe residual strains in TEM samples[10–12] by analyzing higher-order Laue zone (HOLZ) lines. However, for accurate CBED analysis, the samples need to be cooled in a TEM stage to subambient temperatures, a range which is not of practical interest for most of the microelectronic components. In addition, the strains measured are local strains, and the overall stresses can be difficult to assess, especially in a polycrystalline system such as is discussed in this paper. In this paper, we consider the case of single-layer Cu thin films and multilayer Cu interconnect structures used in microelectronic components, as illustrated in Fig. 1.

II. EXPERIMENTAL PROCEDURE

Provided by Freescale Semiconductors (Austin, TX), the as-received test structure consists of electroplated damascene Cu lines integrated with interlayer dielectrics (ILD), Ta diffusion barrier (DB), and SiN_x passivation on a Si substrate (Fig. 1). The Cu lines are 180 nm wide and 300 nm thick, patterned in parallel with a 360-nm pitch. The ILD material is F-doped SiO_2 (F-TEOS), although a low k dielectric material will also be considered in the stress analysis for comparison. The Ta diffusion barrier is 10–20 nm thick, and the SiN_x passivation is 50 nm thick. The thickness of the wafer is 750 μm.

TEM specimens were prepared by disk cutting, mechanical polishing, dimpling, and ion milling. A Fischione 150 Ultrasonic Disk Cutter (Fischione Instruments, Inc., Export, PA) was used to cut a 3-mm disk from the wafer, which was then mechanically polished to about 80 μm in thickness using a diamond lapping film. The sample thickness during lapping was accurately controlled by a Tripod Polisher (SPI Supplies, West Chester, PA). Next, the polished sample was dimpled to about 4 μm thickness using a Fischione 150 Dimpling Grinder, followed by ion milling on both sides with a Fishione1010 ion miller to achieve an electron transparent thickness (~50 nm). The resulting TEM specimen consisted of Cu lines bounded by a diffusion barrier on each side. The diffusion barrier on the bottom side of the Cu has been removed, as well as the passivation and the top dielectric layer. Figure 2 shows a cross-section schematic of the specimen after preparation. Figure 3 shows a TEM image of the Cu lines taken with a JEOL 2010F (Tokyo, Japan) operated at 200 kV. The microstructure exhibits mostly a bamboo grain structure for the 180 nm lines.

To facilitate the stress analysis using a finite element method (FEM), the thickness profile of the TEM specimen was measured by convergent beam electron diffraction in the electron transparent area, and by a Veeco profilometer (Woodbury, NY) away from the electron transparent area. These measurements gave a nearly linear increase in thickness from the electron transparent

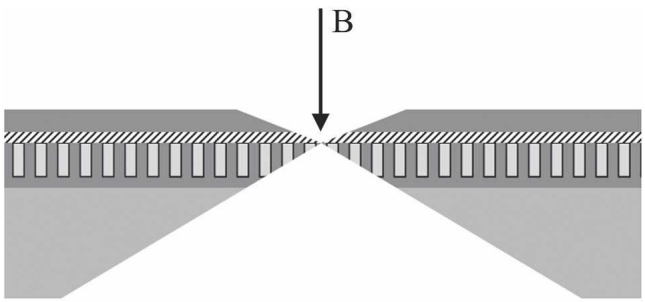

FIG. 2. (a) Schematic cross-sectional view of electron transparent TEM samples. The electron beam direction B is indicated by the arrow.

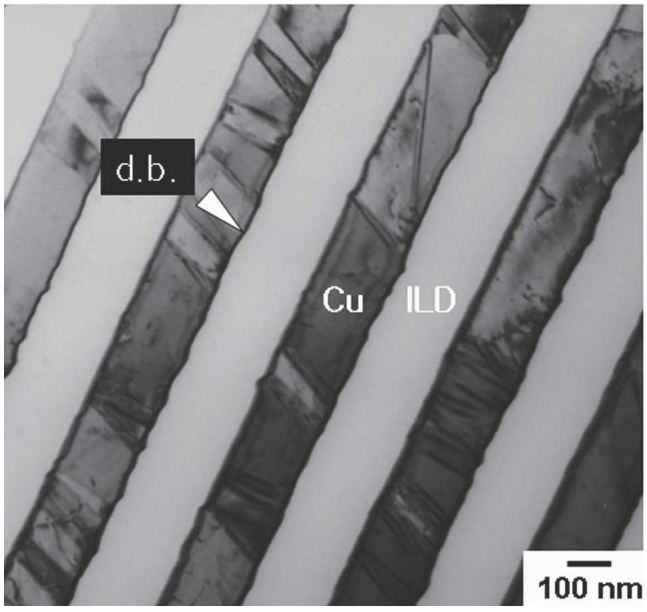

FIG. 3. TEM planar view of 180 nm Cu interconnect lines, showing the diffusion barriers (d.b.) and the interlayer dielectrics (ILD).

area at the center of the specimen, to a distance 150 μm from the edge of the sample. The thickness of the electron transparent area, which is solely composed by Cu was found to be approximately 50 nm.

III. RESULTS AND DISCUSSIONS

We will now examine how the residual stress in the Cu interconnect lines has been altered due to the TEM sample preparation. For the sake of simplicity and because many studies carried out on thin films are performed on single-layer structures, we first consider a model with one homogeneous film on the Si substrate (Fig. 4). The film thickness h_f is set to be 1 μm, which is roughly the total thickness of the multilayer interconnect structure including the Cu lines and the dielectric layer. The substrate thickness h_s is taken to be 80 μm after polishing. The wafer radius R_s is 1500 μm to simulate the 3-mm disk samples used for TEM observations, and the edge width R_g is 150 μm from the profilometry measurements. The thickness and radius of the electron transparent area, h_e and R_e, will be varied in the stress analysis.

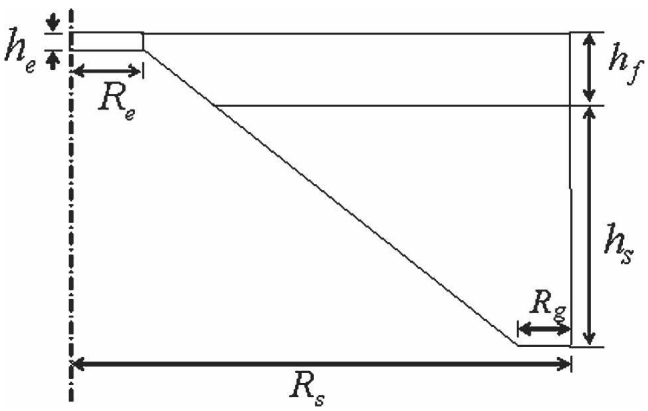

FIG. 4. Axisymmetric FEM model of the TEM specimen.

The stress in the film is introduced by temperature changes, due to differential thermal expansion of the film and the substrate. Since the focus here is the relative changes of stress in the TEM specimen compared with the as-received structure, the exact origin of the stress is not essential. Before sample preparation, both the substrate thickness and the wafer radius are significantly larger than the film thickness. In such a case, the thermally induced stress in the film is given by

$$\sigma_0 = \frac{E_f}{1-\nu_f}(\alpha_s - \alpha_f)\Delta T \quad , \tag{1}$$

where α_s and α_f are the coefficients of thermal expansion for the substrate and the film, respectively, E_f is the Young's modulus of the film, ν_f the Poisson's ratio, and ΔT is the temperature change. Here we assume no plastic yield or stress relaxation in the film.

The stress in Eq. (1) serves as the reference stress that is compared with the stress in the TEM specimen. The relative changes in elastic stress between the as-received and the electron transparent sample can be calculated for any temperature. The stress in the TEM specimens is calculated from an axisymmetric finite element model (FEM) using the commercial package ABAQUS.[13] As illustrated in Fig. 4, the specimen is roller supported along its outer edge and subject to rotational symmetry at its central axis. A relatively fine FEM mesh was used for the film, especially for the electron transparent area. The material properties used in the FEM analyses are listed in Table I. Because of the geometry of the specimen, the stress distribution in the film is generally nonuniform. The average radial stress along the central axis is calculated and plotted in Fig. 5 as a function of the electron transparent thickness h_e with different R_e, for a homogeneous Cu film on a Si substrate. It shows that the relative stress change increases as the thickness h_e decreases. For $h_e = 50$ nm, the average stress at the center is more than twice of the reference stress given in Eq. (1). On the other hand, the radius R_e has less effect on the stress. The

TABLE I. Material properties used for finite element analysis.

	Young's modulus, E (GPa)	Poisson's ratio	CTE (ppm/K)
Si	165	0.22	4.2
Cu	128	0.36	17.0
SiN_x	290	0.27	2.9
TEOS	72	0.20	1.4
SiLK	2.45	0.35	66.0

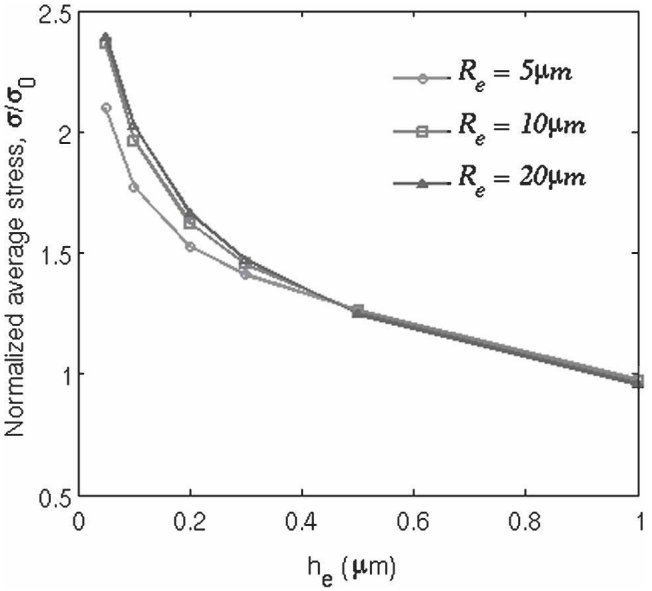

FIG. 5. Average stress as a function of the TEM section thickness for different section radii.

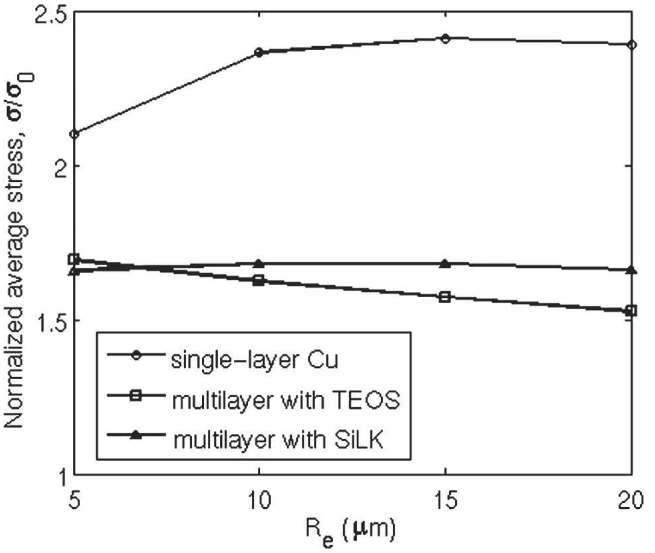

FIG. 6. Comparison of the stresses in multilayer and single-layer models.

enhancement of stress in the electron transparent area can be understood as a result of the interaction between the thin and thick parts of the film. Near the junction of the thin and thick parts, the stress in the film is redistributed so that the total force in the radial direction from the thick part of the film equals that from the thinner part. When $h_e = h_f$, the redistribution is minimal and the stress becomes slightly lower than the reference stress. This is because the removal of the substrate material has reduced the overall stiffness of the substrate that constrains the thermal expansion of the film. Therefore, the stress in the electron transparent area of the film is altered by two competing mechanisms, namely stress amplification due to thickness reduction of the film and stress relaxation due to substrate removal. When the electron transparent thickness is significantly less than the total film thickness, the stress amplification dominates. Otherwise, when the total film thickness is close to the electron transparent thickness, the stress relaxation effect dominates.

Next we consider a multilayer model, replacing the homogeneous film of Fig. 4 with a multilayer comprised, from bottom up, by a dielectric layer (400 nm), a Cu film (300 nm), a SiN_x passivation layer (50 nm) and another dielectric layer (250 nm), with the same total film thickness as in the single-layer model. The overall geometry of the specimen is identical, except that both the SiN_x passivation and dielectric layers are removed from the center region of the specimens, leaving only Cu in the electron transparent area (50 nm thick) of the sample. Figure 6 compares the relative change in the average stress between the single-layer model (for a homogeneous Cu film) and the multilayer model with two different dielectric materials. The thickness of the electron transparent area is now fixed with $h_e = 50$ nm, while the radius R_e varies from 5 to 20 μm. Apparently, the relative stress change in the multilayer model is reduced, mainly due to the relatively low stiffness in the thick part of the multilayer film containing the dielectric materials. It is noted that, while Cu and SiLK have larger coefficients of thermal expansion (CTEs) than Si, TEOS and SiN_x have smaller CTEs. Consequently, the reference stresses in TEOS and SiN_x have the opposite sign of the stresses in Cu and SiLK. This leads to the different trend in Fig. 6 for the multilayer model with TEOS compared to the other two curves. Also interestingly, although the stiffness of SiLK is much lower than TEOS, the relative stress change is comparable to that with TEOS. This is again attributed to the opposite stress sign in TEOS, which partly compensates the stress redistribution in the Cu film. Therefore, the stress state in the multilayer thin films is complicated, depending on the relative stiffness of each layer as well as the coefficients of thermal expansion.

The present stress analysis applied to the geometry of a TEM specimen provides a first understanding of the relative change in the stress states. A further refinement of the analysis would consider patterned Cu lines instead of a continuous Cu film, for which a three-dimensional FEM model is required and the computational cost becomes formidable due to the scale difference between the wafer and individual Cu lines.

IV. CONCLUSIONS

In summary, we have shown that the film stress can be considerably altered in TEM specimens of multilayer

thin films after sample preparation processes. The stress state depends on the geometry as well as the interactions among multiple layers. Although the present analysis is based on linear elasticity and does not account for the detailed microstructure of the films, it provides a qualitative understanding on the mechanisms of stress redistribution. The elastic stresses may be considered as the starting point before any relaxation processes (such as dislocation generation, void formation, or buckling) take place. The results from this work suggest a way to minimize the changes in stress by combining careful stress analysis with the design of the sample geometry. This has important consequences for using in situ TEM as a tool for device reliability analysis. The minimization of the change in stress can be important in allowing correct correlation between in situ TEM work, and the behavior of the material in its bulk state.

ACKNOWLEDGMENTS

The authors would like to thank the Center for Nano and Molecular Science and Technology, the Texas Materials Institute and Freescale Semiconductors for their support of this research. The authors would also like to thank Dr. Martin Gall at Freescale Semiconductors for his useful discussions. R. Huang and H. Mei are grateful for the financial support by National Science Foundation through Grant CMS-0547409.

REFERENCES

1. R.P. Vinci, E.M. Zielinski, and J.C. Bravman: Thermal strain and stress in copper thin films. *Thin Solid Films* **262,** 142 (1995).
2. M.A. Korhonen, P. Borgesen, and C-Y. Li: Mechanisms of stress-induced and electromigration-induced damage in passivated narrow metallizations on rigid substrates. *MRS Bull.* **17**(7) (1992).
3. *Critical Reliability Challenges for the International Technology Roadmap for Semiconductors*, Reliability Technical Advisory Board (RTAB), International SEMATECH, 2003.
4. B. Li, T.D. Sullivan, T.C. Lee, and D. Badami: Reliability challenges for copper interconnects. *Microelectron. Reliabil.* **44,** 365 (2004).
5. Z.H. Shi, D. Onsongo, R. Rai, S.B. Samavedam, and S.K. Banerjee: Hole mobility enhancement and Si cap optimization in nanoscale strained $Si_{1-x}Ge_x$ PMOSFETs. *Solid State Electron.* **48,** 2299 (2004).
6. D. Jawarani, H. Kawasaki, I-S. Yeo, L. Rabenberg, J.P. Stark, and P.S. Ho: In situ transmission-electron-microscopy study of plastic deformation in passivated Al–Cu thin films. *J. Appl. Phys.* **82,** 171 (1997).
7. S.P. Hau-Riege and C.V. Thompson: In situ transmission electron microscope studies of the kinetics of abnormal grain growth in electroplated copper films. *Appl. Phys. Lett.* **76,** 309 (2000).
8. G. Dehm and E. Arzt: In situ TEM study of dislocations in a polycrystalline Cu thin film constrained by a substrate. *Appl. Phys. Lett.* **77,** 1126 (2000).
9. J.H. An and P.J. Ferreira: In situ transmission electron microscopy observations of 1.8 micron and 180 nm Cu interconnects under thermal stresses. *Appl. Phys. Lett.* **89,** 151919 (2006).
10. C.T. Chou, S.C. Anderson, D.J.H. Cockayne, A.Z. Sizorski, and M.R. Vaughan: Surface relaxation of strained heterostructures revealed by Bragg line splitting in LACBED patterns. *Ultramicroscopy* **55,** 334 (1994).
11. F. Houdellier, C. Roucau, and M-J. Casaonve: Convergent beam diffraction for strain determination at the nanoscale. *Microelectron. Eng.* **84,** 464 (2007).
12. J. Nucci, S. Kramer, E. Arzt, and C.A. Volkert: Local strains measured in Al lines during thermal cycling and eletromigration using convergent-beam electron diffraction. *J. Mater. Res.* **20,** 1851 (2005).
13. *ABAQUS User's Manual,* version 6.6, Providence, RI, 2006.